ELSEVIER

Journal of Organometallic Chemistry 655 (2002) 49–54

Journal of Organometallic Chemistry

www.elsevier.com/locate/jorganchem

The reactions of 4,6-dimethyl-2-mercaptopyrimidine with dimetallic compounds: diiron nonacarbonyl and cyclopentadienylmolybedenum tricarbonyl dimer

Fung-E Hong *, Yi-Luen Huang, Pin-Pin Chen, Yu-Chang Chang

Department of Chemistry, National Chung-Hsing University, Taichung 40227, Taiwan, ROC

Received 30 October 2001; received in revised form 15 March 2002; accepted 22 March 2002

Abstract

Treatment of 4,6-dimethyl-2-mercaptopyrimidine with diiron nonacarbonyl at 25 °C in THF, gave two isomeric compounds, $[(\eta^2\text{-}\mu_1\text{-C,N–}C_6H_7N_2)Fe_2(CO)_6(\mu_4\text{-S})Fe_2(CO)_6(\mu_2\text{-S–}SC_6H_7N_2)]$ (**2**) and (**3**). The X-ray structure analysis revealed that the cores of **2** and **3** are $(\mu_4\text{-S})Fe_4$ units with centered spirocyclic forms. On one side of the molecule, one diiron fragment is bridged by a pyrimidyl ligand through its nitrogen and carbon atoms; on the other side, the other diiron fragment is doubly bridged by a pyrimidinethiolate through its sulfur atom. Inter-conversion between **2** and **3** occurred rather slowly at 25 °C in solution; nevertheless, the rate was enhanced in the presence of high pressure of carbon monoxide. A major product, $[(\eta^2\text{-}\mu_1\text{-C,N–}C_6H_7N_2)Fe_2(CO)_6(\mu_4\text{-S})Fe_2(CO)_5(P(OMe)_3)(\mu\text{-S–}SC_6H_7N_2)]$ (**4**), was obtained while **2** was treated with $P(OMe)_3$ in THF at 25 °C for 24 h. In contrast, the reaction of 4,6-dimethyl-2-mercaptopyrimidine with cyclopentadienylmolybedenum tricarbonyl dimer in THF at 50 °C, gave an unimetallic complex, $[(\eta^5\text{-}C_5H_5)Mo(CO)_2(\eta^2\text{-S,N–}SC_6H_7N_2)]$ (**5**). Crystal structure of **5** revealed that the deprotonated mercaptopyrimidine acted as a bidentate ligand.

Keywords: Mercaptopyrimidine; Dimetallic compound; Isomeric forms; μ_4-S centered spirocyclic form; Metal-promoted reaction

1. Introduction

Many transition metal cluster compounds containing bridging sulfido ligand are known. However, transition metal complexes with μ_4-S centered spirocyclic form are rare [1]. In the early report of Le Borgne on reaction of 2-mercaptopyridine with $Fe_3(CO)_{12}$, a complex of formula $[(\eta^2\text{-}\mu_1\text{-C,N–}C_5H_4N)Fe_2(CO)_6(\mu_4\text{-S})Fe_2(CO)_6(\mu_2\text{-S–}SC_5H_4N)]$ (**1**) was characterized by a single-crystal X-ray study [2]. The centered sulfur, a bridging μ_4-S, serves as a six-electron donor [3]. Obviously, the formation of **1** involved both deprotonation of S–H bond and cleavage of S–C bond of thiols.

With more functional groups and substituents, 4,6-dimethyl-2-mercaptopyrimidine, a small variation of 2-mercaptopyridine, was expected to exhibit much versatile bonding capacities toward dimetallic compounds. Here, we will describe some fascinating results from the reaction of 4,6-dimethyl-2-mercaptopyrimidine with diiron nonacarbonyl, $Fe_2(CO)_9$. In addition, the reaction of this thiol with another dimetallic compound, dicyclopentadienylmolybedenum tricarbonyl dimer, $[(\eta^5\text{-}C_6H_5)Mo(CO)_2]_2$, was pursued and result will be presented as well.

2. Results and discussion

The reaction of 4,6-dimethyl-2-mercaptopyrimidine with iron nonacarbonyl, $Fe_2(CO)_9$, at 25 °C for 1 h, yielded two isomeric compounds, $[(\eta^2\text{-}\mu_1\text{-C,N–}C_6H_7N_2)Fe_2(CO)_6(\mu_4\text{-S})Fe_2(CO)_6(\mu_2\text{-S–}SC_6H_7N_2)]$ (**2**) and (**3**) (Scheme 1). The polarities of these two reddish–orange colored compounds are quite different thus makes the separation of them feasible during the chromatographic processes. The isolated yields for **2** and **3** are 33.60 and 7.38%, respectively. Both compounds were characterized by spectroscopic means as well as X-

* Corresponding author. Fax: +886-4-2286-252247.
E-mail address: fehong@dragon.nchu.edu.tw (F.-E. Hong).

0022-328X/02/$ - see front matter
PII: S0022-328X(02)01412-2

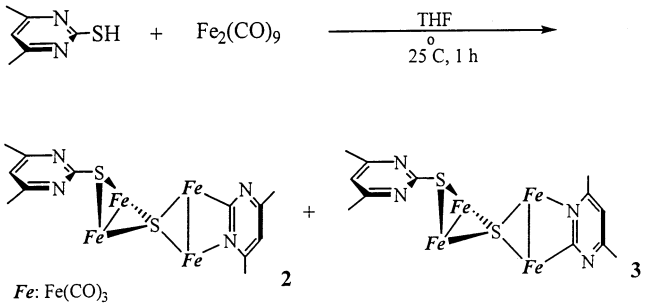

Scheme 1. Formation of conformational isomers of **2** and **3**.

ray crystallographic analyses. Le Borgne did not notice two isomeric forms of **1** in his early work [2].

The crystal structures of **2** and **3** revealed that both forms are having a $(\mu_4\text{-S})Fe_4$ core in a centered spirocyclic shape. They only differ from the placement of the bidentate ligand, $\eta^2\text{-}\mu_2\text{-C,N–}C_6H_7N_2$. The pyrimidinethiolate, $\mu_2\text{-S–}SC_6H_7N_2$, serves as a bridging ligand towards a diiron fragment. Each iron fragment, with three terminal carbonyls, is in a pseudo-octahedral environment. Carbonyls are arranged in eclipse form in each diiron fragment. Two conformational isomers are presented in each unit cell of the crystals (Chart 1). Presumably, ready conversions of the conformational isomers are occurred in solution.

The process of forming **2** and **3** involved both the breaking of the S–C and S–H bond of 4,6-dimethyl-2-mercaptopyrimidine. Three signals, in the ratio of 2:1:1, for the methyl groups were obtained in ^{1}H as well as ^{13}C-NMR for **2** in $CDC1_3$. This is well consistent with its solid-state structure. Interestingly, only two signals, in the ratio of 2:2, for the methyl groups were obtained in ^{1}H-NMR for **3**, probably due to coincidental merger of two methyl signals. Slightly splitting of these two signals was observed in high frequency NMR or changing to d^8-toluene solvent [4]. The variable-temperature ^{1}H-NMR experiment was carried out for **3** over the range of −90 to +40 °C in toluene-d^8 [5]. Each measurement was taken with the increment of 10 °C. While judging the methyl signals in ^{1}H-NMR, only slightly downfield shift, rather than splitting was observed within the experimental range. Therefore, the inter-conversion process between **2** and **3** could not be observed for short monitoring time under this temperature range. Nevertheless, the conversion did occur very slowly in solution at 25 °C for prolonging time. Also, the conversion rate was greatly enhanced in the presence of high pressure of carbon monoxide. Calculated 33% of **3** was converted to **2** when **3** was placed in a high pressure reactor, which was purged with 500 psi CO, in THF and was stirred for 24 h at 25 °C. There was no CO insertion being observed at Fe–C(pyrimidyl) bond of **2** or **3**, as it has been demonstrated elsewhere [6]. A closer look at the structure of either 2 or 3, one find that the formerly expected expansion of the four-membered ring, Fe–N–C–Fe, to a probably five-membered ring, Fe–N–C–C(=O)–Fe, after CO insertion might actually cause severe steric hindrance between the methyl group and the carbonyl groups of the iron center. That may be the main hindrance to prevent the CO insertion process at the Fe–C(pyrimidyl) bond of **2** or **3** (Figs. 1 and 2).

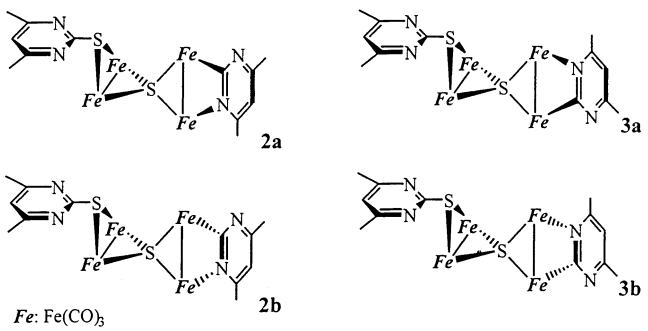

Chart 1. Conformational isomers of **2** and **3**.

A mechanism for the conversion of **3** to **2** or from **2** to **3** in the presence of external ligand is proposed as follows (Scheme 2). Firstly, the entering ligand coordinates to one specific iron center, which is away from the bridging pyrimidyl ligand, of **3** and causes the breaking of the corresponding S–Fe bond. Secondly, a rotation along the remaining S–Fe single bond takes place. Finally, the reversal attack from the bridging sulfur towards the ligand coordinated iron center, at the same time, causes the release of one of the carbonyls. Isomer **2** is formed while the entering ligand is carbon monoxide.

The reaction of **2** with $P(OMe)_3$, at 25 °C in THF for 24 h, yielded a single phosphine ligand substituted product, $[(\eta^2\text{-}\mu_1\text{-C,N–}C_6H_7N_2)Fe_2(CO)_6(\mu_4\text{-S})Fe_2(CO)_5(P(OMe)_3)(\mu\text{-S–}SC_6H_7N_2)]$ (**4**) (Scheme 3). The structural analysis of **4** reveals that the entering phosphine ligand coordinates to one particular iron center, which is away from the bridging pyrimidyl ligand, to avoid the steric hindrance. In the case of a bulky

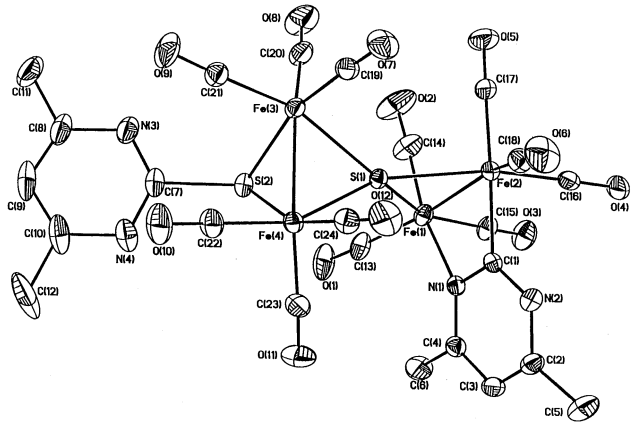

Fig. 1. ORTEP drawing with the numbering scheme of **2**. All hydrogen atoms are omitted for clarity.

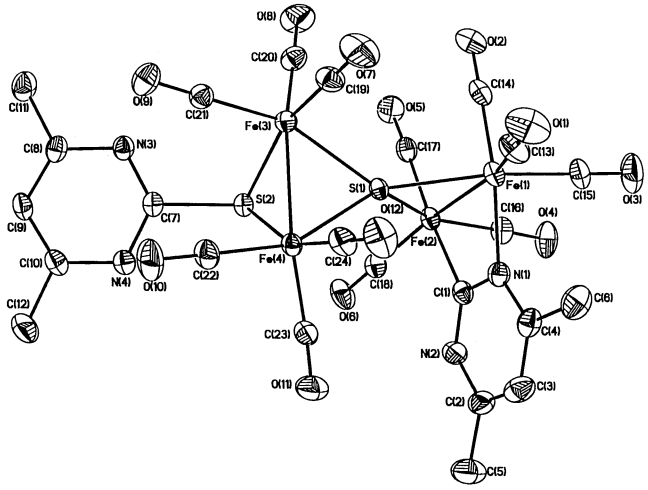

Fig. 2. ORTEP drawing with the numbering scheme of **3**. All hydrogen atoms are omitted for clarity.

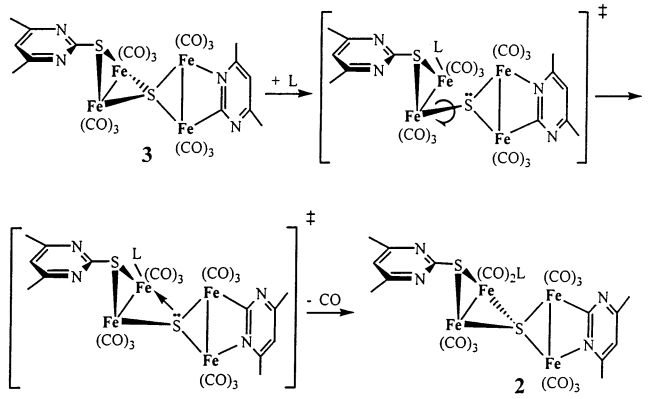

Scheme 2. Proposed mechanism for the conversion of **3** to **2** or from **2** to **3**.

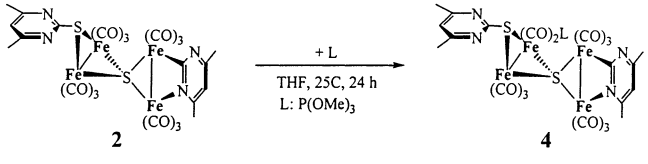

Scheme 3. Ligand substitution of **2** by $P(OMe)_3$.

phosphine like $P(OCH_3)_3$, the rotation through Fe–S single bond in the transition state as proposed in Scheme 2 is not favored due to the steric hindrance between two bulky groups, phosphine and pyrimidyl. Therefore, only the direct lisand substituted product **4**, rather than the isomeric form, was observed. Three signals, in the ratio of 2:1:1, for the methyl groups were obtained in ^1H as well as ^{13}C-NMR for **4**. Two methyl groups of the pyrimidinethiolate ligand are equivalent because of the capability of free rotation of the S–C(pyrimidinethiolate) bond (Fig. 3).

Selected structural parameters of **2**, **3** and **4** were shown in Table 2 for the purpose of comparison. As it has shown in Table 2, the main frameworks for **2** and **3**

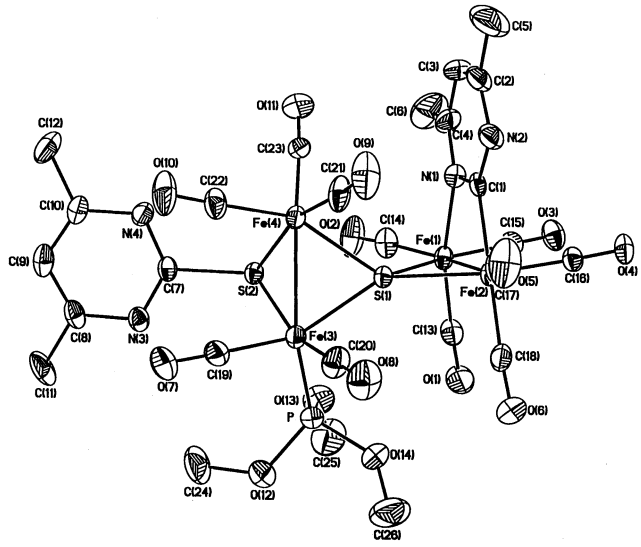

Fig. 3. ORTEP drawing with the numbering scheme of **4**. All hydrogen atoms are omitted for clarity.

are not much different. Because of one of the iron centers is coordinated with a bulky phosphine ligand, $P(OMe)_3$ in **4**, the dihedral angles for **4** are quite different from that of **2** or **3**.

The reaction of 4,6-dimethyl-2-mercaptopyrimidine with cyclopentadienylmolybedenum tricarbonyl dimer, $[(\eta^5\text{-}C_5H_5)Mo(CO_3)]_2$, at 50 °C for 8 h, yielded a unimetallic compound, $[(\eta^5\text{-}C_5H_5)Mo(CO)_2(\eta^2\text{-}S,N\text{–}SC_6H_7N_2)]$ **5** [7] (Scheme 4). The crystal structure of **5** shows that the pyrimidinethiolate acts as a bidentate chelating ligand, that is different from **2** or **3**. It can be seen as compound having a four-legged piano-stool conformation [8]. Four atoms, Mo(1), S(1), C(6), N(1), are almost coplanar. The Mo–Mo bond of $[(\eta^5\text{-}C_5H_5)Mo(CO_3)]_2$, was cleaved at a relatively mild condition under the influence of thiols [9]. The fact that the breaking of S–H bond of mercaptopyrimidine rather than the S–C bond is sensible for forming a relatively stable four-membered ring than the strained three-membered ring in **5** (Fig. 4).

The variable-temperature ^1H-NMR experiment was carried out for **5** in toluene-d^8 over the range of 25–90 °C. Indicates, the methyl signals did not show significant change within the experimental range. The expected Mo–N(pyrimidinethiolate) bond breaking did not occur in this monitoring temperature range. The fact that there was no noticeable change for further reaction of **5** with $HC{\equiv}CSiMe_3$ also supports the observation.

3. Summary

In this work, the reactivity of mercaptopyrimidine towards dimetallic compounds such as $Fe_2(CO)_9$ and $[CPMo(CO)_3]_2$.were explored. The results show that this

Table 1
Crystal data of **2**–**5**

	2	**3**	**4**	**5**
Empirical formula	$C_{24}H_{14}Fe_4N_4O_{12}S_2$	$C_{24}H_{14}Fe_4N_4O_{12}S_2$	$C_{26}H_{23}Fe_4N_4O_{14}PS_2$	$C_{13}H_{12}MoN_2O_2S$
Formula weight	837.91	837.91	933.97	356.25
Crystal system	Monoclinic	Monoclinic	Triclinic	Monoclinic
Space group	$P2_1/n$	$P2_1/n$	$P\bar{1}$	$P2_1/c$
a (Å)	21.6104(13)	9.2263(17)	9.1994(10)	8.4276(13)
b (Å)	15.6771(9)	23.071(4)	10.7630(13)	24.192(4)
c (Å)	9.7014(6)	15.530(3)	20.975(2)	14.326(2)
α (°)	90	90	96.105(2)	90
β (°)	92.3370(10)	95.429(4)	96.377(2)	105.251(3)
γ (°)	90	90	113.590(2)	90
V (Å^3)	3284.0(3)	3290.9(10)	1865.3(4)	2817.9(8)
Z	4	4	2	8
D_{calc} (Mg m^{-3})	1.695	1.691	1.663	1.679
λ (Mo–K$_\alpha$) (Å)	0.71073	0.71073	0.71073	0.71073
μ (mm^{-1})	1.922	1.918	1.746	1.077
2θ range, (°)	1.61–26.03	1.77–26.12	1.98–26.05	1.68–26.00
Observed reflections [$F > 4\sigma(F)$]	4105	3975	3200	3764
No. of refined parameters	415	415	460	343
R_1 [a] for significant reflections	0.0385	0.0417	0.0575	0.0417
wR_2 [b] for significant reflections	0.1020	0.1029	0.1303	0.1107
Goodness-of-fit [c]	0.917	0.907	0.806	0.844

[a] $R_1 = |\Sigma\ (|F_o| - |F_c|)/|\Sigma\ F_o||$.
[b] $wR_2 = \{\Sigma\ [w(F_o^2 - F_o^2)^2/\Sigma\ [w(F_o^2)^2]\}^{1/2}$; $w = 0.10$ for **2**, **5**, **4**, **5**.
[c] Goodness-of-fit $= \{\Sigma\ [w(F_o^2 - F_c^2)^2/(N_{reflections} - N_{parameters})]^{1/2}$.

Table 2
Comparison of selected structural parameters of **2**–**4**

	2	**3**	**4**
Bond length (Å)			
Fe(1)–Fe(2)	2.5920(8)	2.5842(9)	2.5710(14)
Fe(3)–Fe(4)	2.5319(8)	2.5247(10)	2.5356(17)
S(l)–Fe(1)	2.2494(11)	2.2361(13)	2.260(2)
S(1)–Fe(2)	2.2196(11)	2.2186(12)	2.2323(19)
S(1)–Fe(3)	2.2531(11)	2.2391(13)	2.255(2)
S(1)–Fe(4)	2.2500(11)	2.2502(12)	2.2628(19)
S(2)–Fe(3)	2.2572(12)	2.2583(13)	2.261(2)
S(2)–Fe(4)	2.2614(12)	2.2699(13)	2.270(2)
Fe(1)–N(1)	2.006(3)	1.997(4)	2.008(7)
Fe(2)–C(1)	1.960(4)	1.966(5)	1.921(8)
Fe(3)–P			2.186(3)
Bond angle (°)			
Fe(1)–S(1)–Fe(2)	70.90(4)	70.91(4)	69.81(6)
Fe(3)–S(l)–Fe(4)	68.42(3)	68.44(4)	68.28(6)
Fe(4)–S(2)–Fe(3)	68.16(4)	67.77(4)	68.05(6)
Fe(l–N(1)–C(l)	105.7(2)	104.6(3)	104.5(5)
N(1)–C(1)–Fe(2)	110.8(3)	111.0(3)	110.6(5)
C(1)–Fe(2)–Fe(1)	71.39(11)	71.15(14)	72.6(2)
Fe(2)–Fe(1)–N(1)	72.13(9)	73.27(11)	72.2(2)
Dihedral angle (°)			
Planel–Plane2 [a]	98.11	96.4	100.3
Planet–Plane3	82.5	83.9	94.8
Plane3–Plane4	97.7	95.3	85.0

[a] Plane 1: S(2), Fe(3), Fe(4); Plane 2: S(l), Fe(3), Fe(4); Plane 3: S(1), Fe(1), Fe(2); Plane 4: Fe(l), Fe(2), C(1), N(1).

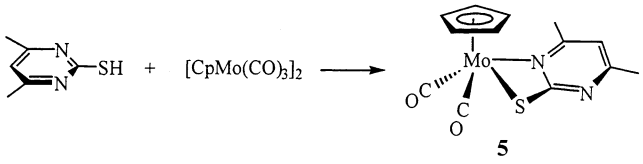

Scheme 4. Formation of $[(\eta^5\text{-}C_5H_5)Mo(CO)_2(\eta^2\text{-}S,N\text{–}SC_6H_7N_2)]$ **5**.

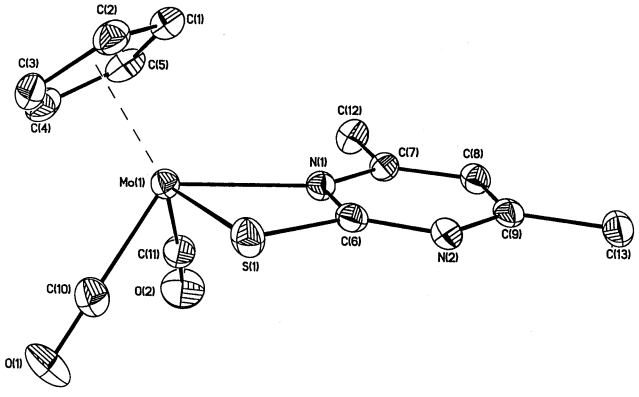

Fig. 4. Molecular structure of one of two independent molecules of **5**. All hydrogen atoms are omitted for clarity.

ligand could be incorporated into iron clusters through the form of bridging pyrimidinethiolate or pyrimidyl ligand and forming complexes containing (μ_4-S)Fe_4 unit with a centered spirocyclic geometry. One of the

carbonyl ligands of this iron cluster could be replaced by a $P(OMe)_3$ ligand while the main structure remains the same. In contrast to the case of diiron, only unimetallic complex was obtained from the reaction of ligand with molybedenum dimer.

4. Experimental

4.1. General

All operations were performed in a nitrogen-flushed glove box or in a vacuum system. Freshly distilled solvents were used. All processes of separations of the products were performed by Centrifugal Thin-Layer Chromatography (TLC, Chromatotron, Harrison model 8924). ^{1}H and ^{13}C-NMR spectra were recorded (Varian-VXR-300S spectrometer) at 300.00 and 75.46 MHz, respectively; chemical shifts are reported in ppm relative to internal TMS. ^{1}H-NMR spectra of variable temperature experiments were recorded by the same machine. Some other routine ^{1}H-NMR spectra were recorded at Gemini-200 spectrometer at 200.00 MHz or Varian-400 spectrometer at 400.00 MHz. IR spectra of solution in CH_2Cl_2, or of solid state in KBr were recorded on a Hitachi 270-30 spectrometer. Mass spectra were recorded on JOEL JMS-SX/SX 102A GC/MS/MS spectrometer. Elemental analyses were recorded on Heraeus CHN–O–S-Rapid. Accurate elemental analyses were precluded for some of the following compounds probably due to their chemical labilities.

4.1.1. Preparation of 2 and 3

Into a 100 cm^3 flask was placed iron nonacarbonyl, $Fe_2(CO)_9$, (1.0000 g, 2.7488 mmol) and 4,6-dimethyl-2-mercaptopyrimidine (0.3854 g, 2.7488 mmol) with 20 ml of THF. The solution was stirred at room temperature (r.t.) during the next 1 h. Subsequently, the resulting reddish orange solution was filtered through a small amount of silica gel. Purification with centrifugal thin-layer chromatography (CTLC) was carried out. The first band, $[(\eta^2\text{-}\mu_1\text{-}C,N\text{–}C_6H_7N_2)Fe_2(CO)_6(\mu_4\text{-}S)Fe_2(CO)_6\text{-}(\mu_2\text{-}S\text{–}SC_6H_7N_2)]$ (**2**), in the yield of 33.60% (0.3870 g, 0.4619 mmol) was eluted by mixture solvent (C_6H_{14}–$CH_2Cl_2 = 1{:}1$). The second band containing **3**, was eluted by polar mixture solvent (CH_2Cl_2–MeOH = 3:1) in the yield of 7.38% (0.0850 g, 0.1014 mmol).

4.1.2. Characterization of 2

^{1}H-NMR ($CDCl_3$, δ ppm): 2.28 (s, 3H, CH_3), 2.38 (s, 3H, CH_3), 2.40 (s, 6H, CH_3), 6.60 (s, 1H, CH), 6.82 (s, 1H, CH); ^{13}C-NMR: 23.42 (2C, CH_3), 23.68 (1C, CH_3), 24.00 (1C, CH_3), 117.35, 117.73, 118.41, 164.58, 164.87, 167.25, 171.84 (1C, 2C, 1C, 1C, 1C, 1C, 1C, pyrimidine), 206.83, 208.04, 213.71 (3C, 6C, 3C, CO); IR(KBr): ν_{co} 1988(m), 2038(m). Anal. Calc. for **2**: N, 6.69; C, 34.40; H, 1.68. Found: N, 6.41; C, 33.76; H, 1.90%. M.S.: m/z 839 ($P^+ = M+1$).

4.1.3. Characterization of 3

^{1}H-NMR($CDCl_3$, δ ppm): 2.32 (s, 3H, CH_3), 2.33 (s, 3H, CH_3), 2.39 (s, 6H, CH_3), 6.59 (s, 1H, CH), 6.81 (s, 1H, CH); ^{13}C-NMR: 23.41 (2C, CH_3), 23.82 (2C, CH_3), 117.33, 117.72, 118.36, 164.56, 165.38, 167.23, 171.68 (1C, 1C, 2C, 1C, 1C, 1C, 1C, pyrimidine), 206.72, 207.16, 207.89, 212.96 (3C, 3C, 3C, 3C, CO); IR(KBr): ν_{co} 1990(s), 2041(s). Anal. Calc. for **3**: N, 6.69; C, 34.40; H, 1.68. Found: N, 6.08; C, 32.94; H, 2.64%. M.S.: m/z 839 ($P^+ = M+1$).

4.1.4. Conversion of 2–3

Into a 50 cm^3 stainless Parr high pressure reactor was placed **3** (0.2915 g, 0.3482 mmol) with 20 ml of THF and was purged with 500 psi CO. The solution was stirred for 24 h at 25 °C. Purification with centrifugal thin-layer chromatography (CTLC) was carried out. Calculated 33% of **3** was converted to **2** (0.0962 g, 0.1149 mmol).

4.1.5. Preparation of 4

Into a 100 cm^3 flask was placed **2** (0.8000 g, 0.9548 mmol) and $P(OMe)_3$ (0.1126 ml, 0.9548 mmol) with 20 ml of THF. The solution was stirred at r.t. for 24 h. The procedures of further purification of the resulting dark orange solution are as mentioned previously. The first band was eluted by CH_2Cl_2. The isolated yield of **4** is 21.4% (0.1911 g, 0.2046 mmol).

4.1.6. Characterization of 4

^{1}H-NMR ($CDCl_3$, δ ppm): 2.28 (s, 3H, CH_3), 2.36 (s, 6H, CH_3), 2.39 (s, 3H, CH_3), 3.77 (d, $J_{PH} = 10.8$, 9H, CH_3), 6.60 (s, 1H, CH), 6.75 (s, 1H, CH); ^{13}C-NMR: 23.41 (2C, CH_3), 23.65 (1C, CH_3), 24.03 (1C, CH_3), 52.79 ($J_{PC} = 189$ Hz), 117.01, 117.54, 117.67, 163.88, 164.53, 166.54, 173.56 (1C, 1C, 2C, 1C, 1C, 1C, 1C, pyrimidine), 207.67, 209.57, 214.33 (3C, 6C, 3C, CO). Anal. Calc. for (**5**): N, 6.20; C, 34.58; H, 2.57. Found: N, 5.68; C, 34.36; H, 3.03%.

4.1.7. Preparation 5

A mixture of $[(\eta^5\text{-}C_5H_5)Mo(CO)_3]_2$ (0.4838 g, 1.0000 mmol) and 4,6-dimethyl-2-mercaptopyrimidine (0.2804 g, 2.0000 mmol) in 20 ml THF was stirred overnight under 50 °C. In 6–8 h the solution color changed from burgundy red to dark orange. The solvent was removed in vacuo, the residue was dissolved in minimum CH_2Cl_2 and purified with Centrifugal thin-layer chromatography (CTLC). The first eluted band was identified as unreacted $[(\eta^5\text{-}C_5H_5)Mo(CO)_3]_2$. The second band, $[(\eta^5\text{-}C_5H_5)Mo(CO)_2(\eta^2\text{-}S,N\text{–}SC_6H_7N_2)]$ (**5**), was eluted by CH_2Cl_2 and recrystallized from mixture solvent

(C_6H_{14}–CH_2Cl_2 = 1:1) to give the orange–red crystals. The yield of **5** is 86.00% (0.3035 g, 0.8600 mmol).

4.1.8. Characterization of **5**

^{1}H-NMR ($CDCl_3$, δ ppm): 2.31 (s, 3H, CH_3), 2.36 (s, 3H, CH_3), 5.56 (s, 5H, Cp), 6.52 (s, 1H, pyrimidine); ^{13}C-NMR: 22.71 (s, CH_3), 23.88 (s, CH_3), 94.72 (s, Cp), 114.10, 168.64, 180.93 (1C, 1C, 1C, pyrimidine), 252.44, 259.08 (1C, 1C, CO). Anal. Calc. for **5**: C, 43.80; H, 3.37.. Found: C, 42.21; H, 4.10%. MS (FAB): *m*/*z* 358 (P^+ = M+3); IR(KBr): ν_{co} 1951(s), 1859(s).

5. X-ray crystallographic studies

Suitable crystals of **2**, **3**, **4** and **5** were sealed in thin-walled glass capillaries under nitrogen atmosphere and mounted on a Bruker AXS SMART 1000 diffractometer. Intensity data were collected in 1350 frames with increasing ω (width of 0.3° per frame). The absorption correction was based on the symmetry equivalent reflections using SADABS program. The space group determination was based on a check of the Laue symmetry and systematic absences, and was confirmed using the structure solution. The structure was solved by direct methods using a SHELXTL package. All non-H atoms were located from successive Fourier maps and hydrogen atoms were refined using a riding model. Anisotropic thermal parameters were used for all non-H atoms, and fixed isotropic parameters were used for H atoms. Crystallographic data of **2**, **3**, **4** and **5** are summarized in Table 1.

6. Supplementary material

Crystallographic data for the structural analysis have been deposited with the Cambridge Crystallographic Data Center, CCDC Nos. 181490–181493 for compounds **2**–**5**. Copies of this information may be obtained free of charge from the Director, CCDC, 12 Union Road, Cambridge CB2 1EZ, UK (Fax: +44-1223-336033; e-mail: deposit@ccdc.cam.ac.uk or www: http://www.ccdc.cam.ac.uk).

Acknowledgements

We are grateful to the National Research Council of the R.O.C. (Grant NSC 90-2113-M-005-021) for financially supporting this research.

References

[1] (a) Z.-X. Wang, H. Zhao, Z.-Y. Zhou, X.-G. Zhou, J. Organomet. Chem. 599 (2000) 256;
(b) Z.-X. Wang, C.-S. Jia, Z.-Y. Zhou, X.-G. Zhou, J. Organomet. Chem. 601 (2000) 108;
(c) Z.-X. Wang, H. Zhao, Z.-Y. Zhou, X.-G. Zhou, J. Organomet. Chem. 595 (2000) 158;
(d) L.-C. Song, Q.-M. Hu, H.-T. Fan, B.-W. Sun, M.-Y. Tang, Organometallics 19 (2000) 3909;
(e) H.-B. Zheng, S.-B. Miao, Z.-X. Wang, Z.-Y. Zhou, X.-G. Zhou, Polyhedron 19 (2000) 713;
(f) H. Egold, D. Schwarze, M. Schraa, U. Florke, J. Chem. Soc. Dalton Trans. (2000) 4385;
(g) L.-C. Song, G.-L. Lu, Q.-M. Hu, H.-T. Fan, Y. Chen, J. Sun, Organometallics 18 (1999) 3258;
(h) Z.-X. Wang, C.-S. Jia, Z.-Y. Zhou, X.-G. Zhou, J. Organomet. Chem. 580 (1999) 201;
(i) L.-C. Song, X.-D. Qin, Q.-M. Hu, X.-Y. Huang, Organometallics 17 (1998) 5437;
(j) R.E. Marsh, Acta Crystallogr. Sect. B 51 (1995) 897;
(k) B.R. Cockerton, A.J. Deeming, Polyhedron 13 (1994) 2085;
(l) A.J. Deeming, K.I. Hardcastle, M. Karim, Inorg. Chem. 31 (1992) 4792;
(m) K.I. Hardcastle, B.R. Cockerton, A.J. Deeming, M. Karim, J. Chem. Soc. Dalton Trans. 186 (1992) 1607;
(n) L.-C. Song, Q.-M. Hu, L.-Y. Zhang, H. Wang, Z.-Y. Zhou, L. Liu, J. Organomet. Chem. 412 (1991) C19;
(o) L.-C. Song, M. Kadiata, J.-T. Wang, R.-J. Wang, H.-G. Wang, J. Organomet. Chem. 340 (1988) 239;
(p) H.G. Raubenheimer, G.J. Kruger, A.A. Lombard, J. Organomet. Chem. 323 (1987) 385;
(q) B.I. Kolobkov, N.S. Nametkin, V.D. Tyurin, A.I. Nekhaev, G.G. Aleksandrov, J. Organomet. Chem. 301 (1986) 349;
(r) A. Shaver, O. Lopez, D.N. Harpp, Inorg. Chim. Acta 119 (1986) 13;
(s) C. Glidewell, A.R. Hyde, Inorg. Chim. Acta 87 (1984) L15;
(t) R.D. Adams, D.F. Foust, Organometallics 2 (1983) 323;
(u) H. Patin, G. Mignani, C. Mahe, J.-Y. Le Marouille, A. Benoit, D. Grandiean, J. Organomet. Chem. 210 (1981) C1;
(v) S.C. Carleton, F.G. Kennedy, S.A.R. Knox, J. Chem. Soc. Dalton Trans. (1981) 2230;
(w) J.M. Coleman, A. Wojcicki, P.J. Pollick, L.F. Dahl, Inorg. Chem. 6 (1967) 1236.
[2] G. Le Borgne, D. Grandjean, J. Organomet. Chem. 92 (1975) 381.
[3] R.D. Adams, D.F. Foust, Organometallics 2 (1983) 323.
[4] Two signals are resolved at 600 MHz NMR.
[5] Compound **4** starts to decompose above 40 °C. Therefore, the reaction could not carry out beyond that temperature.
[6] A recent report appeared on CO insertion into Co-arene bond taking place under 1 bar of CO atmosphere. See H.-F. Klein, S. Schneider, M. He, U. Floerke, H.-J. Haupt, Eur. J. Inorg. Chem. (2000) 2295.
[7] Y. Shi, G. Cheng, S. Lu, H. Guo, Q. Wu, X. Huang, N. Hu, J. Organomet. Chem. 455 (1993) 115.
[8] R.H. Crabtree, The Organometallic Chemistry of the Transition Metals, 2nd ed. (Chapter 5), John Wiley & Sons, Inc, New York, 1994.
[9] It always takes a much more severe reaction condition to get [(η^5-C_5H_5)$Mo(CO)_2$]$_2$ to react.